EnM
ENDOCRINOLOGY AND METABOLISM

Original Article

Endocrinol Metab 2024;39:127-139
https://doi.org/10.3803/EnM.2023.1826
pISSN 2093-596X · eISSN 2093-5978

FoxO6-Mediated TXNIP Induces Lipid Accumulation in the Liver through NLRP3 Inflammasome Activation

Mi Eun Kim[1], Jun Sik Lee[1], Tae Won Kim[2], Min Hi Park[2], Dae Hyun Kim[3]

[1]Department of Life Sciences, Chosun University College of Natural Science, Gwangju; [2]Department of Pharmacy, Kyungsung University College of Pharmacy, Busan; [3]Department of Food Science & Technology, Pusan National University College of Natural Resources and Life Science, Miryang, Korea

Background: Hepatic steatosis, which involves the excessive accumulation of lipid droplets in hepatocytes, presents a significant global health concern due to its association with obesity and metabolic disorders. Inflammation plays a crucial role in the progression of hepatic steatosis; however, the precise molecular mechanisms responsible for this process remain unknown.

Methods: This study investigated the involvement of the nucleotide-binding oligomerization domain-like receptor pyrin domain-containing-3 (NLRP3) inflammasome and the forkhead box O6 (FoxO6) transcription factor in the pathogenesis of hepatic steatosis. We monitored the NLRP3 inflammasome and lipogenesis in mice overexpressing the constitutively active (CA)-FoxO6 allele and FoxO6-null mice. In an *in vitro* study, we administered palmitate to liver cells overexpressing CA-FoxO6 and measured changes in lipid metabolism.

Results: We administered palmitate treatment to clarify the mechanisms through which FoxO6 activates cytokine interleukin (IL)-1β through the NLRP3 inflammasome. The initial experiments revealed that dephosphorylation led to palmitate-induced FoxO6 transcriptional activity. Further palmitate experiments showed increased expression of IL-1β and the hepatic NLRP3 inflammasome complex, including adaptor protein apoptotic speck protein containing a caspase recruitment domain (ASC) and pro-caspase-1. Furthermore, thioredoxin-interacting protein (TXNIP), a key regulator of cellular redox conditions upstream of the NLRP3 inflammasome, was induced by FoxO6 in the liver and HepG2 cells.

Conclusion: The findings of this study shed light on the molecular mechanisms underpinning the FoxO6-NLRP3 inflammasome axis in promoting inflammation and lipid accumulation in the liver.

Keywords: FoxO6; TXNIP; NLRP3 inflammasome; Interleukin-1beta; Hepatic steatosis

Received: 15 September 2023, **Revised:** 2 November 2023,
Accepted: 13 November 2023

Corresponding authors: Min Hi Park
Department of Pharmacy, Kyungsung University College of Pharmacy, 309 Suyeong-ro, Nam-gu, Busan 48434, Korea
Tel: +82-51-663-4884, **Fax:** +82-51-663-4809, **E-mail:** parkmh@ks.ac.kr

Dae Hyun Kim
Department of Food Science & Technology, Pusan National University College of Natural Resources and Life Science, 1268-50 Samnangjin-ro, Samnangjin-eup, Miryang 50463, Korea
Tel: +82-55-350-5355, **Fax:** +82-55-350-5359, **E-mail:** bioimmune@hanmail.net

INTRODUCTION

Forkhead box O (FoxO) transcription factors regulate the target genes of cellular metabolic pathways and play an important role in the oxidative stress response, cell death, and cell cycle [1,2]. FoxO is involved in modulating the expression of genes involved in combating insulin resistance, and molecular modifications of FoxO, including ubiquitination, methylation, acetylation, and phosphorylation, play a role in those processes. For instance, FoxO is phosphorylated by protein kinase B (also known as Akt) in response to insulin and several other growth factors, which allows it to be translocated to the cytoplasm from the nucleus [2-4]. Lower levels of growth factor signaling activate FoxO, since FoxO stops being inhibited by Akt, while FoxO is activated through the c-Jun N terminal kinase pathway in the presence of elevated intracellular levels of reactive oxygen species and certain fatty acids (palmitate) [5,6].

Insulin resistance and low-grade inflammation constitute two key components that function interdependently in type 2 diabetes and obesity. In the former condition, peripheral tissues exhibit a significantly diminished response to normal plasma insulin levels, whereas in the latter condition, proinflammatory cytokines are produced at markedly elevated levels. The causal relationship between chronic low-grade inflammation and the development of insulin resistance has yet to be definitively established, but the association between these two pathological traits implies a crosstalk mechanism in which the abnormal production of inflammatory cytokines is linked to the onset of insulin resistance in obese individuals and, eventually, type 2 diabetes [7,8]. Recent studies have reported that FoxO1 mediates the impact of insulin on the expression of target genes in peripheral cells [2,3,9]. However, selectively inhibiting the activity of FoxO6, another member of the FoxO family, in the liver of insulin-resistant mice improved lipid metabolism via the suppression of both hepatic lipogenesis and the excessive production of very low-density lipoprotein assembled from triglycerides. In contrast, the activation of FoxO6 was linked to metabolic disorders such as hepatic steatosis, hyperlipidemia, and insulin resistance [10]. FoxO inhibition has been found to efficiently curb excessive hepatic glucose production and improve glycemic control in diabetes [11]. We aimed to investigate this relationship because the mechanisms linking inflammation to insulin resistance are not understood completely. In addition, previous research has shown that patients with type 2 diabetes and mice that consumed a high-fat diet produced interleukin (IL)-1β after obesity-induced "danger signals" prompted the activation of the nucleotide-binding oligomerization domain (NOD)-like receptor pyrin domain-containing-3 (NLRP3) inflammasome [12]. Elevated serum levels of proinflammatory cytokines are integrally involved in the pathogenesis of metabolic disorders, and novel anti-inflammatory therapies have been suggested to treat these conditions [13]. However, the specific inflammation-related signaling pathways that give rise to the abovementioned metabolic abnormalities have yet to be identified.

Under inflammatory conditions, several NOD-like receptors, including NLRP3, the adaptor protein apoptotic speck protein containing a caspase recruitment domain (ASC), and pro-caspase-1, are recruited by certain pattern recognition proteins and combine to form molecular platforms known as inflammasomes. Inflammasomes mediate the catalytic activation of caspase-1, after which the proinflammatory cytokines IL-18 and IL-1β are released [14]. IL-1β is a major inflammatory cytokine, and research has suggested its involvement in metabolic disorders such as diabetes [15]. Inflammatory stimuli, including both endogenous danger-associated molecules and the products of microbes, trigger the production of IL-1β, initially in its inactive form (pro-IL-1β). The cleavage of pro-IL-1β into the bioactive IL-1β is catalyzed by caspase-1, which in turn is activated from pro-caspase-1 by the inflammasomes [16].

Thioredoxin-interacting protein (TXNIP) is the product of an early response gene that shows a high level of induced expression under hyperglycemic conditions and diabetes [17,18]. Zhou et al. [19] found that TXNIP and vitamin D3 upregulated protein 1 (VDUP1) were integrally involved in the activation of caspase-1 in response to high glucose levels in murine β-cells through direct interactions with the NLRP3 inflammasome. Numerous cell types, including adipocytes, endothelial cells, pancreatic β-cells, and skeletal myocytes, express TXNIP, and TXNIP functions as an endogenous inhibitor of thioredoxin, a protein that scavenges reactive oxygen species [20,21]. The impairment of thioredoxin activity by FoxO1 increased the expression of TXNIP-induced reactive oxygen species [22]. An increase in VDUP1 expression contributed to cellular senescence establishment by FoxO3a at the transcriptional and post-transcriptional levels [19]. Furthermore, individuals with type 2 diabetes demonstrated elevated TXNIP levels [21], and glucose-6-phosphate induces TXNIP expression through an intracellular transcriptional complex consisting of MondoA and Max-like protein X [23]. However, the role of FoxO6 in the TXNIP-induced activation of the NLRP3 inflammasome has yet to be clearly established.

In this study, we documented the FoxO6 dephosphorylation

process in HepG2 cells and mouse liver, showing how FoxO6 and NLRP3 inflammasome activities change during inflammation, with potential implications for the pathogenesis of hepatic steatosis.

METHODS

Animals

Male C57BL/6J mice aged 6 weeks were purchased from the Jackson Laboratory (Bar Harbor, ME, USA). The mice were kept in sterile cages with a 12-hour light/dark cycle, and they received standard rodent chow and water *ad libitum*. The C57BL/6J mice were randomly allocated to two groups. In one group, the mice received an intravenous injection (into the tail) of an adenoviral vector containing the FoxO6 constitutively active allele (AdV-FoxO6-CA), which converted Ser184 to Ala184 in the FoxO6 polypeptide chain. The other group of mice received an intravenous injection of an AdV-null vector into the tail. Both injections involved a dose of 1.5×10^{11} plaque-forming units (pfu) per kilogram of body weight. After a 2-week period following the AdV-FoxO6-CA injection, mice were fasted for 24 hours before being sacrificed. Venous blood samples were then obtained from their tails to determine blood glucose levels, as previously described.

To generate homozygous knockout mice (FoxO6-KO), $FoxO6^{+/-}$ heterozygous mice received standard rodent chow or a high-fat diet (fat content, 60 kcal%; Research Diets Inc., New Brunswick, NJ, USA), according to the group they were in, as well as water *ad libitum*. The mice were kept in sterile cages with a 12-hour light/dark cycle. We obtained livers from FoxO6-KO mice from the University of Pittsburgh Medical Center (Pittsburgh, PA, USA).

All experiments were approved and carried out in accordance with the regulations of the Chosun University Care and Use Committee (CIACUC2022-A0022). All mice were housed at the Chosun University Specific-Pathogen-Free (SPF) Animal Care Unit.

Cell culture system

HepG2 cells (human hepatocellular carcinoma) were obtained from American Type Culture Collection (Manassas, VA, USA, USA). The cells were cultured in Dulbecco's Modified Eagle Medium (DMEM, Nissui Co., Tokyo, Japan) supplemented with 0.25 μg/mL amphotericin B, 233.6 mg/mL glutamine, and 10% heat-inactivated (56°C, 30 minutes) fetal bovine serum (Gibco, Grand Island, NY, USA). The cells were maintained at 37°C in a 5% CO_2 humidified atmosphere.

Materials

We obtained all chemical reagents from Sigma (St. Louis, MO, USA), except as otherwise noted. The compound 2',7'-dichlorodihydrofluorescein was obtained from Molecular Probes Inc. (Eugene, OR, USA). We obtained Western blotting detection reagents from Amersham (Bucks, UK); RNAzol B from TEL-TEST Inc. (Friendwood, TX, USA); antibodies against TXNIP, IL-1β, caspase-1, ASC, NLRP3, total-Akt, p-Akt, histone H1, β-actin, and α-tubulin from Santa Cruz Biotechnology (Dallas, TX, USA); antibodies against FoxO6 and p-FoxO6 (Ser184) from Dr. HH Dong (University of Pittsburgh, Pittsburgh, PA, USA); horseradish peroxidase-conjugated anti-rabbit immunoglobulin G (IgG), and horseradish peroxidase-conjugated anti-mouse IgG antibodies from Amersham; horseradish peroxidase-conjugated anti-sheep/goat IgG from donkey from Serotec (Oxford, UK); and polyvinylidene difluoride (PVDF) membranes from Millipore Corporation (Billerica, MA, USA).

Nuclear extract preparation

Frozen mouse liver tissues (0.2 to 0.4 μg) were rinsed in phosphate-buffered saline (PBS) and then transferred to a Dounce tissue grinder (Wheaton, DWK Life Sciences, Millville, NJ, USA). Solution A (10 mM 4-(2-hydroxyethyl)-1-piperazine ethane sulfonic acid [HEPES] at a pH of 7.9, with 0.5 mM phenylmethylsulfonyl fluoride [PMSF], 1 mM dithiothreitol [DTT], 0.1 mM ethylene glycol tetraacetic acid [EGTA], 0.1 mM ethylene glycol-bis(β-aminoethyl ether)-N,N,N',N'-tetraacetic acid [EDTA], and 10 mM potassium chloride) was added at a concentration of 2.5 mL/g of tissue. The tissue was homogenized into a liquid mass using five pestle strokes. Five additional strokes were performed for homogenization after NP-40 (0.5%) was added. We transferred the homogenates to Eppendorf tubes and centrifuged them in a microcentrifuge (Beckman, Brea, CA, USA) for 1 minute.

The supernatant predominantly contained content from the cytoplasm. The nuclear pellet was obtained by adding 400 μL of solution C (20 mM HEPES at a pH of 7.9, with 0.4 M sodium chloride [NaCl] and 1 mM of PMSF, DTT, EGTA, and EDTA). After thorough stirring, the tubes were placed on a small rotatory shaker for 15 minutes. The mixture was subsequently centrifuged in a microcentrifuge at 12,000 rpm for 3 minutes. The supernatant, which contained nuclear proteins, was then carefully removed and transferred to a fresh tube, followed by storage at –80ºC until Western blotting was performed. A bicinchoninic acid assay (Sigma) was used to determine the protein content.

Western blotting

Western blotting was performed as described elsewhere [24]. The homogenized samples were mixed with a gel-loading buffer (125 mM Tris-Cl, 4% sodium dodecyl sulfate [SDS], 10% 2-mercaptoethanol at a pH of 6.8, 0.2% bromophenol blue) at a 1:1 ratio and boiled for 5 minutes. SDS-polyacrylamide gel electrophoresis (PAGE) was performed to separate the total protein-equivalents for each sample, following the description of Laemmli [25], and a semi-dry transfer system (15 V for 1 hour) was used to transfer the proteins to a PVDF membrane. We immediately placed the membrane into a blocking buffer (1% non-fat milk) with 10 mM Tris at a pH of 7.5, 100 mM NaCl, and 0.1% Tween-20. Blocking was conducted at room temperature for 1 hour. Incubation of the membrane with a specific primary antibody was conducted at 25ºC for 1 hour, followed by incubation with a horseradish peroxidase-conjugated secondary antibody at 25ºC for 1 hour. Enhanced chemiluminescence was used to detect antibody labeling, following the manufacturer's instructions. Pre-stained protein markers were used to determine the molecular weight.

Immunoprecipitation of cell extracts

Cell extracts were immunoprecipitated in a buffer containing 40 mM Tris-HCl (pH 7.6), 120 mM NaCl, 20 mM NaF, 20 mM β-glycerophosphate, 5 mM EDTA, 2 mM sodium orthovanadate, 1 mM PMSF, 0.1% NP40, leupeptin (2 μg/mL), pepstatin A (1 μg/mL), and aprotinin (1 μg/mL). Aliquots of cell extracts were centrifuged at 12,000 ×*g* at 4ºC for 15 minutes, incubated overnight at 4ºC with the corresponding antibody, and then incubated overnight at 4ºC with a 50% protein A-agarose slurry. The immunoprecipitates were washed thrice with immunoprecipitation buffer, and the immunoprecipitated proteins were then analyzed using SDS-PAGE and Western blotting, as described above.

Chromatin immunoprecipitation assay

Chromatin immunoprecipitation (ChIP) was used to investigate the interactions between FoxO6 and the TXNIP promoter DNA. HepG2 cells (2×10^5 cells) were transfected with pGH11 in the presence of the FoxO6 vector at a multiplicity of infection (MOI) of 100 pfu/cell in triplicate. After 24 hours of incubation, a ChIP assay (Upstate Biotechnology, Lake Placid, NY, USA) was performed using the anti-FoxO6 antibody. Immunoblot assays with the rabbit anti-FoxO6 antibody were used to analyze the immunoprecipitates, and polymerase chain reaction (PCR) was used to detect coimmunoprecipitated DNA by means of TXNIP promoter-specific primers (forward 5′-CACGCGCCA-CAGCGATCTCACTGA-3′, reverse 5′-AGATCCGATCTC-CACAAGCACTCC-3′) that flank the FoxO6 consensus site (-3/-214 nt) within the human TXNIP promoter.

Small interfering RNA-mediated gene silencing

TXNIP was knocked down in HepG2 cells using scrambled or TXNIP small interfering RNAs (siRNAs) purchased from IDT (Coralville, IA, USA). Transfection was performed using the Lipofectamine 2000 reagent (Invitrogen, Grand Island, NY, USA). Cells were treated with scrambled or TXNIP-siRNA Lipofectamine complexes (20 nM) in Opti-MEM (Invitrogen) without serum. Following 4 hours of incubation, we replaced the transfection medium with fresh medium. This was followed by another 48 hours of incubation. During this time, the cells were treated with an adenoviral vector containing FoxO6 at the indicated times.

Transfection and luciferase assay

IL-1β activity was estimated using an IL-1β-luciferase vector (University of Pittsburgh) that contained a specific binding sequence for FoxO6. Transfection was performed using Lipofectamine 2000 (Invitrogen). Briefly, 1×10^4 cells/well were seeded in 48-well plates. Once approximately 40% confluence was achieved, the cells were treated with DNA/Lipofectamine 2000 complexes (1 μg/μL) in 500 μL of normal medium (with 10% serum) for 24 hours, then treated with adenovirus-FoxO6 (100 MOI), or adenovirus FoxO6-siRNA (100 MOI) at 24 hours after transfection. Subsequently, palmitate (500 μM) was added for 8 hours. The cells were then washed with PBS and subjected to the Steady-Glo Luciferase Assay System (Promega, Madison, WI, USA). A luminometer was used to measure luciferase activity (GENious, TECAN, Salzburg, Austria).

RNA isolation and real-time RT-PCR

RNA was isolated from liver cells (20 mg) and HepG2 cells (approximately 2×10^6 cells) using the RNeasy Mini Kit (QIAGEN, Valencia, CA, USA). Real-time quantitative reverse-transcription PCR (qRT-PCR) with SYBR Green was conducted to quantify mRNA concentrations in a CFX Connect System (Bio-Rad Laboratories Inc., Hercules, CA, USA). The primers are presented in Supplemental Tables S1, S2. All primers were purchased from Integrated DNA Technologies (Coralville, IA, USA).

Serum cytokine measurements

Cytokine levels were measured utilizing the Luminex multiplex

analysis system (Millipore). Kits from Bioassay Systems (Hayward, CA, USA) were used to analyze serum glucose levels. Insulin concentrations were measured using a specific kit (Shibayagi, Shibukawa, Japan).

Immunofluorescence

HepG2 cells were seeded at 1×10^4 cells/well in 12-well plates, incubated for 24 hours, fixed in 4% paraformaldehyde solution (15 minutes at room temperature), washed with PBS buffer, blocked with 3% normal goat serum (Gibco), and immunostained using rabbit anti-TXNIP antibody (1:1,000 dilution; Santa Cruz) at 4°C overnight. Next, we washed the cells with Tris-buffered saline and incubated them for 3 hours in the presence of anti-rabbit IgG labeled with Alexa Fluor 488 (1:200; Invitrogen). Immunostaining with Hoechst 33342 (1:1,000; Invitrogen) was conducted to visualize the cell nuclei, and TXNIP was determined by confocal laser scanning microscopy (TCS SP2, Leica, Wetzler, Germany).

Hepatic lipid content

Liver tissue samples (20 mg) underwent homogenization in 400 μL of HPLC-grade acetone. After incubation overnight with agitation at room temperature, 50 μL-aliquots of acetone-extracted lipid suspensions were utilized to calculate triglyceride concentrations via the triglyceride kit (Bioassay Systems). Hepatic lipid content was expressed as milligrams of triglycerides per gram of total liver proteins.

Histological analysis

Oil Red O staining was performed as described elsewhere to visualize lipid accumulation, with formazan-treated cells or frozen tissues at an optimal cutting temperature.

Statistical analysis

One-way analysis of variance (ANOVA) was used to analyze differences among the three or more groups. Differences in the means of individual groups were assessed using the Bonferroni *post hoc* test. The Student's *t* test was used to analyze the differences between two groups. Results are expressed as the mean±standard error of the mean. *P* values <0.05 were considered to indicate statistical significance.

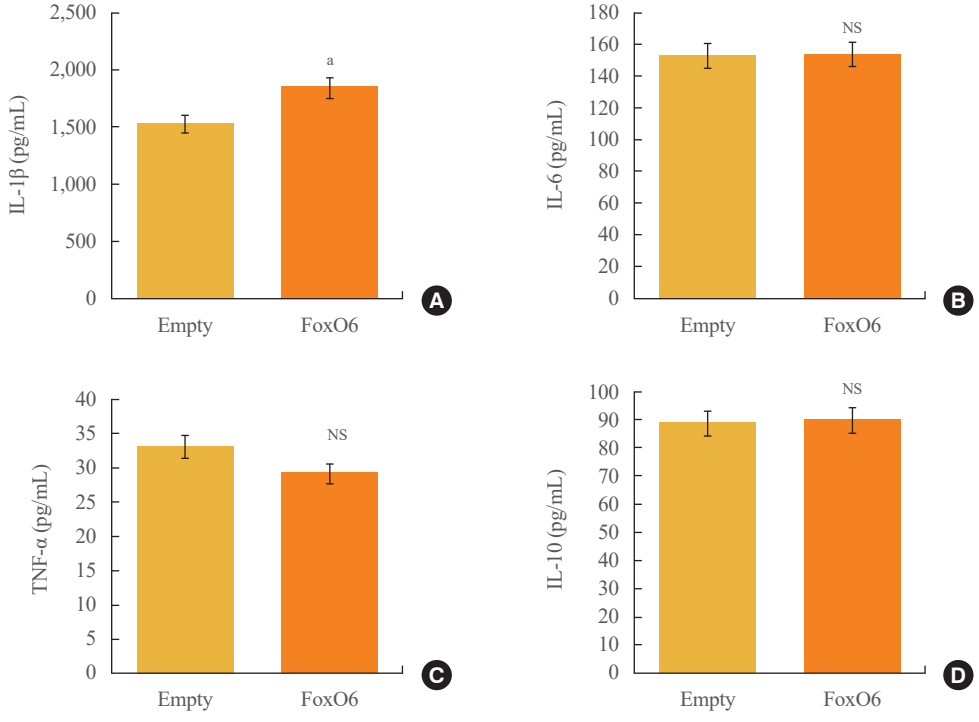

Fig. 1. Effects of forkhead box O6 (FoxO6) on cytokine production. Serum levels of pro-cytokines in mice injected with either constitutively active form of FoxO6 (FoxO6-CA) or null adenoviral vectors, assessed over a period of 13 days: enzyme-linked immunosorbent assay (ELISA) of (A) interleukin (IL)-1β, (B) IL-6, (C) tumor necrosis factor α (TNF-α), and (D) IL-10 ($n=5$ in each group). Three experiments were run for each protein, which yielded similar results; a single representative result is shown here for each protein. NS, not significant. [a]$P<0.01$ vs. the results obtained using the empty adenovirus vector by paired *t* test.

Date availability statement

The datasets supporting the findings of the current study are available from the corresponding author upon reasonable request.

RESULTS

FoxO6 and cytokine production in FoxO6-overexpressing mouse liver

The production of proinflammatory cytokines is dysregulated in obesity and type 2 diabetes. To elucidate the molecular underpinnings of this proinflammatory cytokine production, we investigated the impact of FoxO6 on hepatic cytokine production in mice following injection with a viral vector encoding FoxO6. As depicted in Fig. 1, administration of FoxO6 led to a significant increase in circulating IL-1β without affecting the levels of other cytokines, such as tumor necrosis factor α, IL-6, or IL-10. We verified that FoxO6 was active in the liver, as this transgenic mouse model exhibited liver-specific expression of a constitutively active form of FoxO6 (FoxO6-CA), with no detectable expression in other tissues like adipose or muscle tissue (Supplemental Fig. S1). These findings underscore the role of FoxO6 in the regulation of IL-1β *in vivo* (Fig. 1). Because FoxO6 is associated with abnormal levels of IL-1β, our study concentrated on delineating the molecular mechanisms by which FoxO6 increases IL-1β production.

FoxO6 activation regulates lipid accumulation and NLRP3 inflammasome in mouse liver

To investigate the potential role of FoxO6 in connecting the NLRP3 inflammasome with abnormal IL-1β expression, we examined inflammasome and IL-1β expression in mice following

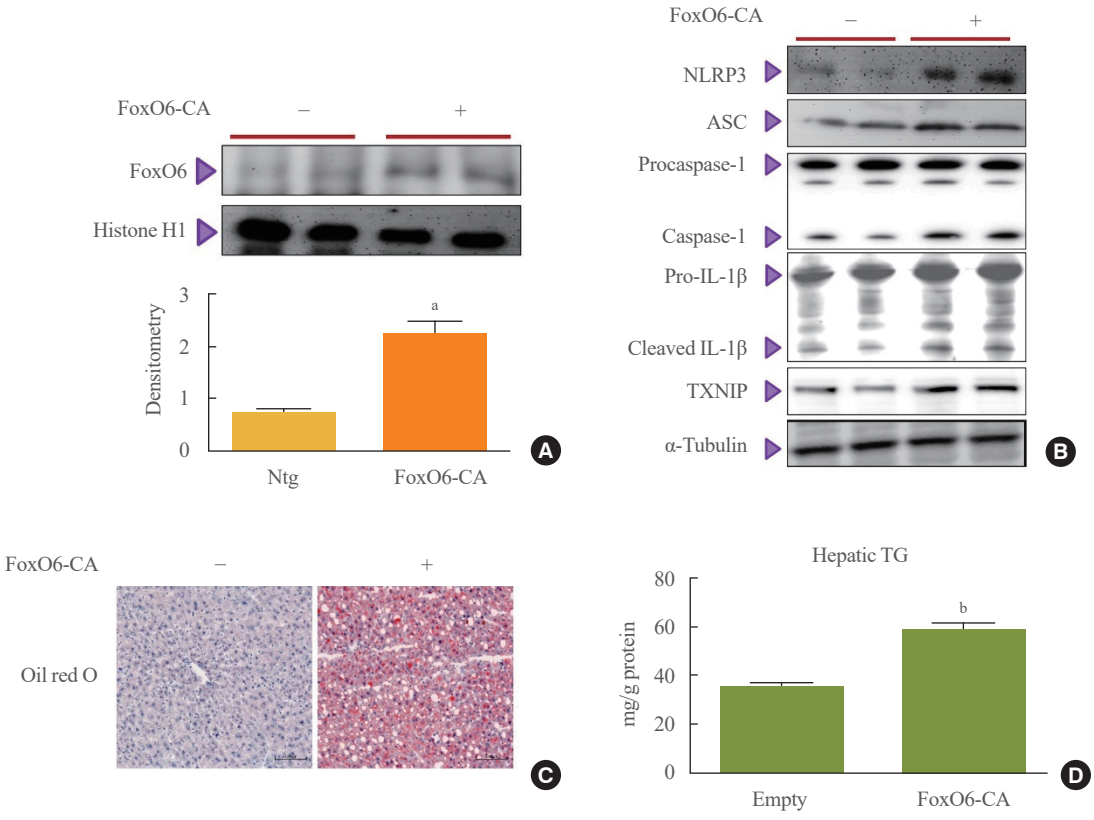

Fig. 2. Forkhead box O6 (FoxO6) regulates nucleotide-binding oligomerization domain-like receptor pyrin domain-containing-3 (NLRP3) inflammasome and lipid accumulation in the liver of mice injected with an adenoviral vector expressing FoxO6. (A) Western blotting was used to detect FoxO6 in the nuclear extracts (20 μg of protein) of liver tissues. Bars in densitometry data represent mean±standard error, and significance was determined using the unpaired test non-trangenic (Ntg). (B) FoxO6 activated the NLRP3 inflammasome genes. Western blotting was used to detect NLRP3, apoptotic speck protein containing a caspase recruitment domain (ASC), caspase-1, interleukin (IL)-1β, and thioredoxin-interacting protein (TXNIP) in cytoplasmic extracts (20 μg of protein) from the liver. (C) Livers were stained with Oil Red O to visualize lipid accumulation (bar=100 μm). (D) Triglyceride levels in hepatic tissues. FoxO6-CA, constitutively active form of FoxO6. [a]$P<0.01$ vs. non-transgenic ($n=3$ each); [b]$P<0.001$ vs. empty vector virus by paired t test.

injection with a FoxO6-CA virus vector. Mice received intravenous injections of either an AdV-FoxO6-CA or an AdV-null vector, after which inflammasome expression levels were measured. Injection with FoxO6-CA was followed by a marked increase in FoxO6 expression in the livers of the treated mice (Fig. 2A). This increase was associated with elevated levels of NLRP3, ASC, and caspase-1 (Fig. 2B), which are three critical components of the inflammasome complex. Additionally, hepatic IL-1β and TXNIP expression were upregulated in the mice treated with FoxO6 (Fig. 2B). Histological analysis using Oil Red O staining also showed greater lipid accumulation in the livers of the FoxO6-CA group compared to the control group (Fig. 2C). In line with these findings, liver triglyceride levels were significantly higher in the FoxO6-CA group (Fig. 2D).

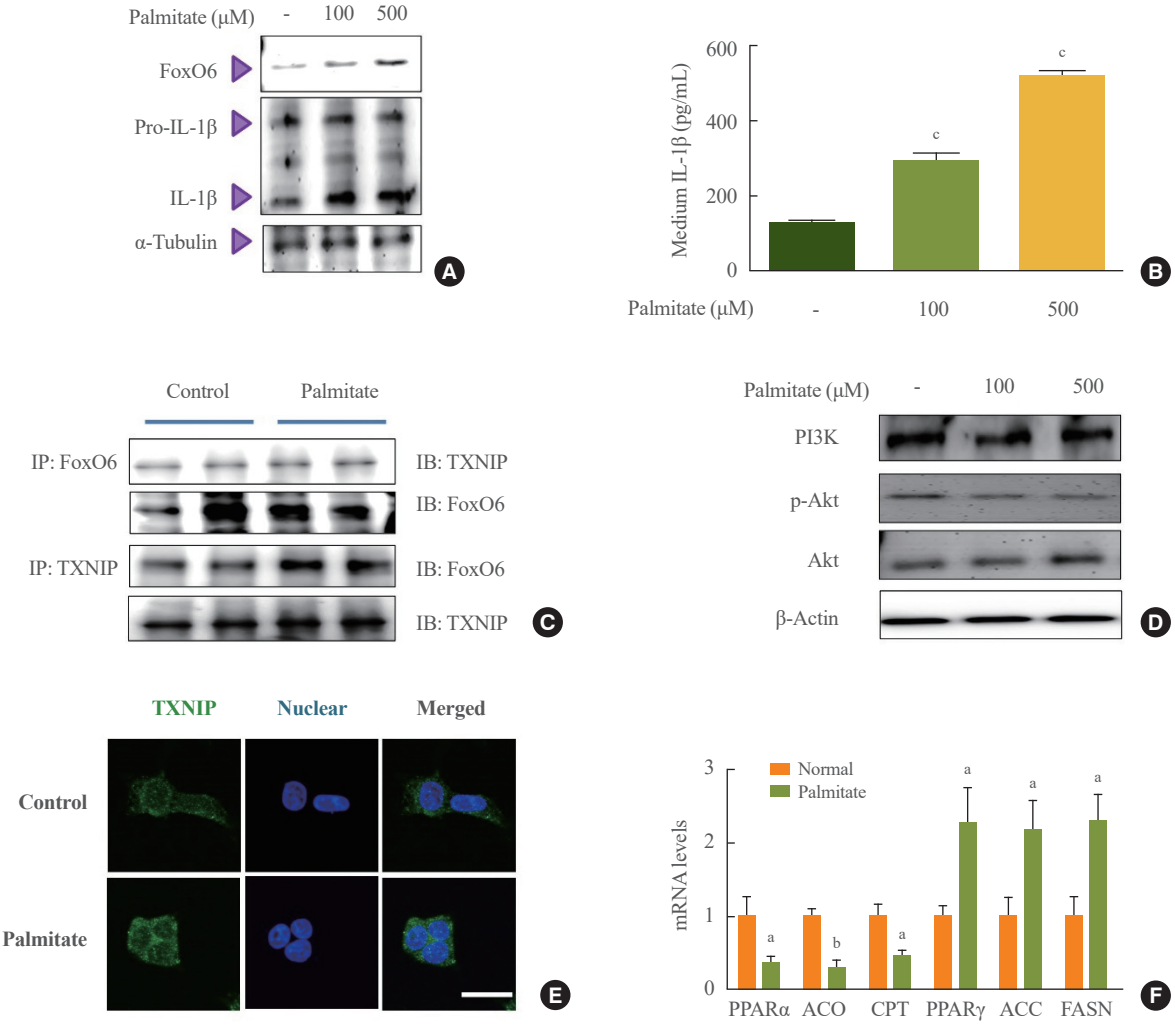

Fig. 3. Interaction between forkhead box O6 (FoxO6) and thioredoxin-interacting protein (TXNIP) induced interleukin (IL)-1β in palmitate-treated HepG2 cells. HepG2 cells were treated with palmitate at various concentrations, and FoxO6 levels were determined by Western blotting. Samples loaded on gels were probed with α-tubulin. (A) Levels of FoxO6 and IL-1β noticeably increased after treatment with 100 and 500 μM palmitate. (B) Effects of palmitate on IL-1β production. The conditioned medium from the experiment in (A) was used for the determination of IL-1β levels. (C) Western blotting showed that immunoprecipitated FoxO6 and TXNIP were physically associated with each other. (D) Levels of phosphoinositide 3-kinase (PI3K), phosphorylated protein kinase B (p-Akt), and total-Akt were noticeably diminished after treatment with 100 and 500 μM palmitate. (E) HepG2 cells were treated with palmitate (500 μM) for 24 hours. Cells were immunostained using rabbit anti-TXNIP antibody followed by immunoglobulin G conjugated with fluorescein isothiocyanate (green) (bar=50 μm). (F) β-Oxidation and lipogenesis genes were subjected to real-time quantitative reverse-transcription polymerase chain reaction analysis. IP, immunoprecipitation; IB, immunoblotting; PPARα, peroxisome proliferator-activated receptor alpha; ACO, acyl-coA oxidase; CPT, carnitine palmitoyltransferase; PPARγ, peroxisome proliferator-activated receptor gamma; ACC, acetyl-coA carboxylase; FASN, fatty acid synthase. $^{a}P<0.05$ and $^{b}P<0.01$ vs. normal by paired *t* test; $^{c}P<0.001$ vs. vehicle by one-way analysis of variance (ANOVA) with Tukey's *post hoc* test.

Association of FoxO6 with TXNIP in palmitate-induced lipid accumulation

To investigate the molecular events that lead to increased FoxO6 expression in HepG2 cells in response to palmitate, we assessed FoxO6 levels using Western blot analysis. Treatment of HepG2 cells with palmitate at concentrations of 100 and 500 μM in serum-free media for 24 hours resulted in a significant elevation of FoxO6 protein levels 24 hours post-treatment (Fig. 3A). Additionally, we explored the effect of palmitate on the cytokine IL-1β (Fig. 3B). The concentration of IL-1β in the medium significantly increased in a dose-dependent manner following palmitate exposure. Similarly, exposing liver cells to high glucose concentrations of 30 mM for durations ranging from 1 to 24 hours produced comparable effects (Supplemental Fig. S2). Immunoprecipitation studies revealed a palmitate-induced interaction between FoxO6 and TXNIP (Fig. 3C). Reduced growth factor signaling leads to FoxO activation due to the loss of Akt-mediated FoxO inhibition, which is also observed with elevated levels of certain fatty acids, such as palmitate. In this study, treatment of HepG2 cells with palmitate at concentrations ranging from 100 to 500 μM for 24 hours resulted in a notable decrease in p-Akt protein levels (Fig. 3D). Treatment with 500 μM palmitate led to a significant translocation of TXNIP to the cytoplasm, as determined by immunostaining (Fig. 3E). This was accompanied by increased mRNA expression of lipogenesis genes and decreased mRNA levels of β-oxidation genes, as quantified by quantitative PCR (qPCR) (Fig. 3F).

Palmitate as a mediator of the FoxO6-induced NLRP3 inflammasome in HepG2 cells

The transcriptional activities of FoxO family proteins are known to increase in response to reduced insulin levels [3]. To test the hypothesis that FoxO6 activates the IL-1β gene, we investigated the nuclear translocation of FoxO6 in HepG2 cells under inflammatory conditions. This was done by treating cells infected with a FoxO6 virus with either 0 or 500 μM palmitate. As shown in Fig. 4A, cells treated with 500 μM palmitate and FoxO6 vectors showed a marked increase in FoxO6 expression. Moreover, the activation of FoxO6 by palmitate in the presence of FoxO6 vectors led to an upregulation of NLRP3 inflammasome gene expression (Fig. 4B). This upsurge in NLRP3 inflammasome levels further corroborates the observed increase in triglyceride content in the FoxO6 and palmitate-treated groups (Fig. 4C).

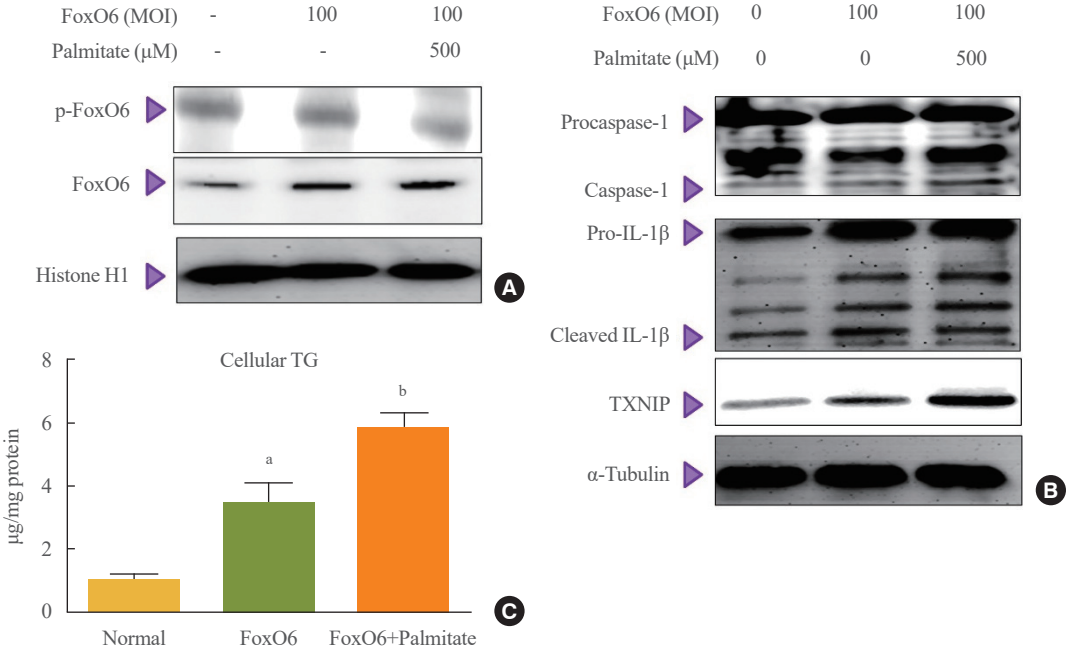

Fig. 4. Palmitate-induced forkhead box O6 (FoxO6) regulated the nucleotide-binding oligomerization domain-like receptor pyrin domain-containing-3 (NLRP3) inflammasome in HepG2 cells. (A) Phosphorylated FoxO6 (p-FoxO6) and total-FoxO6 expression in nuclear. (B) Cytosolic levels of thioredoxin-interacting protein (TXNIP), caspase-1, and interleukin (IL)-1β noticeably increased in FoxO6-transfected (100 multiplicity of infection [MOI]) cells after treatment with 500 μM palmitate. (C) Triglyceride levels in liver cells. [a]$P<0.01$ vs. empty vector virus; [b]$P<0.05$ vs. FoxO6 virus by one-way analysis of variance (ANOVA) with Tukey's *post hoc* test.

IL-1β activation in response to TXNIP-FoxO6 binding

Hepatic oxidative stress is related to TXNIP, which inhibits thioredoxin-1 and -2 in the cytosol and mitochondria, respectively [26]. TXNIP has been identified as a promising therapeutic target for conditions such as hepatic ischemia-reperfusion injury [27], hyperglycemia [28], and acute liver failure. A recent study found that TXNIP may link oxidative stress to inflammasome activation [19]. Furthermore, the introduction of palmitate has been shown to increase the expression of NLRP3 in cultured hepatic stellate cells and hepatocytes [29].

To further explore the importance of FoxO6 in the inflammasome, we employed an siRNA-mediated gene expression approach to knock down TXNIP in HepG2 cells. This was achieved by treating the cells with TXNIP-siRNA. We observed

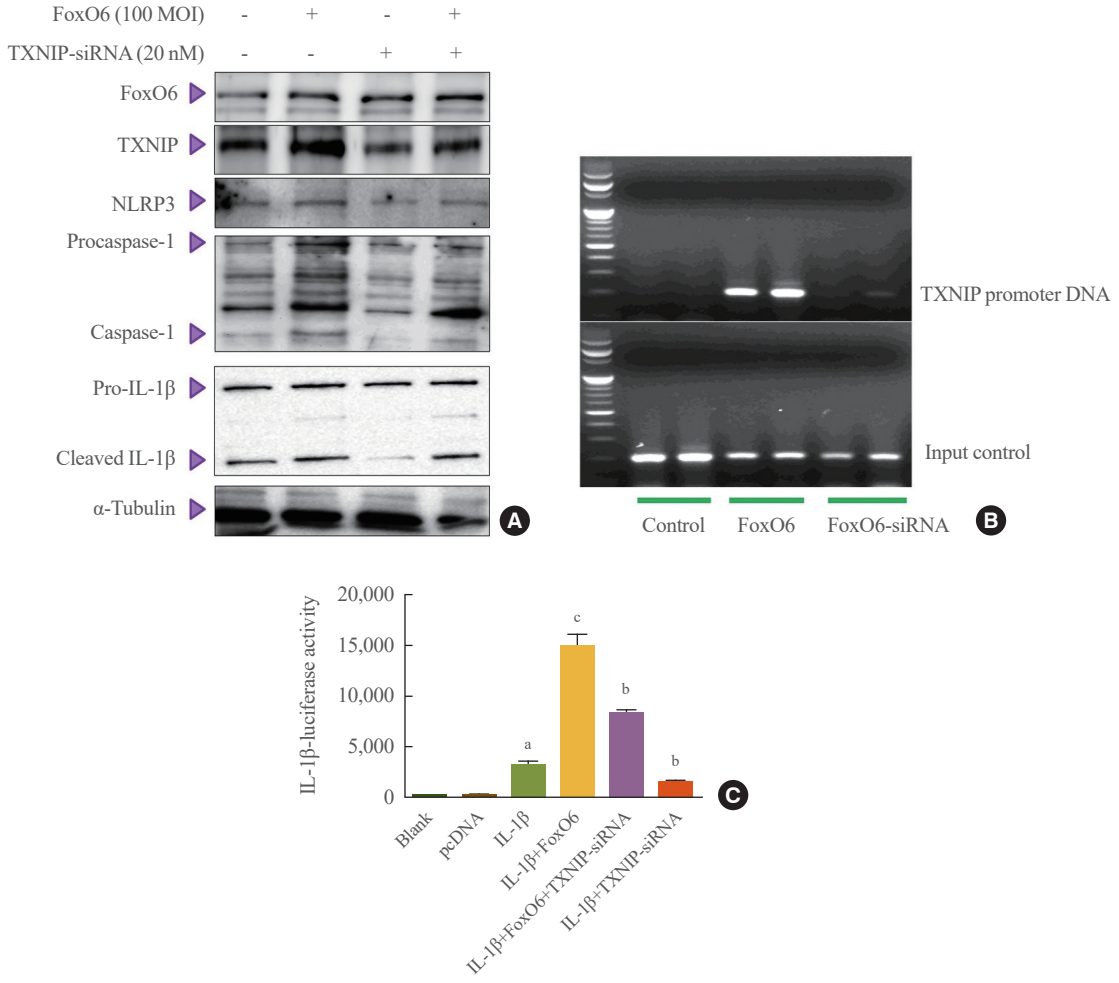

Fig. 5. Forkhead box O6 (FoxO6)-induced thioredoxin-interacting protein (TXNIP) regulated the nucleotide-binding oligomerization domain-like receptor pyrin domain-containing-3 (NLRP3) inflammasome. (A) Pre-treated (1 day) with or without TXNIP-small interfering RNA (siRNA; 20 nM), and then stimulated with FoxO6 (100 multiplicity of infection [MOI]) in cells, and analyzed by Western blotting. (B) FoxO6 bound to the TXNIP promoter in HepG2 cells transfected with a vector containing FoxO6 (100 MOI) or FoxO6-siRNA (100 MOI). After incubation for 24 hours, the cells were subjected to a chromatin immunoprecipitation (ChIP) assay using rabbit pre-immune immunoglobulin G (lanes 1, 2) or anti-FoxO6 antibody (lanes 3–6). The immunoprecipitates were subjected to polymerase chain reaction using the TXNIP promoter. (C) Effect of wild-type FoxO6 with or without TXNIP-siRNA (20 nM) on the activity of the interleukin (IL)-1β promoter. HepG2 cells in 48-well microplates were transduced with adenoviral vector (AdV)-FoxO6, TXNIP-siRNA (20 nM), or control AdV-null vectors at a fixed dose (MOI, 100 pfu/cell), followed by transfection with 0.5 μg of pcDNA and IL-1β DNA in the culture medium. After incubation for 24 hours, the cells were harvested and treated with palmitate (500 μM); luciferase and β-galactosidase activities were determined 8 hours after palmitate treatment. The relative luciferase activity was calculated based on the IL-1β-luciferase/β-galactosidase activity ratio. The data are expressed as mean±standard error of the mean. [a]$P<0.001$ vs. pcDNA treated cells; [b]$P<0.01$, [c]$P<0.001$ vs. IL-1β DNA treated cells by one-way analysis of variance (ANOVA) with Tukey's *post hoc* test.

that levels of NLRP3 inflammasome genes increased with FoxO6 expression but decreased upon treatment with TXNIP-siRNA (Fig. 5A). Subsequently, we investigated FoxO6's ability to promote TXNIP expression in HepG2 cells. ChIP assays revealed that FoxO6 was associated with binding to and activation of the TXNIP promoter (Fig. 5B). These assays were conducted on HepG2 cells transduced with vectors either empty, containing FoxO6, or containing TXNIP-siRNA. Specifically, FoxO6 showed an association with the TXNIP promoter DNA in cells transduced with FoxO6, an association not detected in cells transduced with the empty vector. Conversely, FoxO6 did not associate with the TXNIP promoter DNA in cells transduced with FoxO6-siRNA (Fig. 5B). Additionally, TXNIP was found to be associated with activity at the IL-1β promoter, as demonstrated by IL-1β luciferase assays (Fig. 5C) in cells transduced with the empty vector, the FoxO6-containing vector, and the TXNIP-siRNA-containing vector. FoxO6 was associated with the IL-1β promoter DNA in TXNIP-transfected cells, and this association not observed in the empty-vector-transduced HepG2 cells.

Change in the NLRP3 inflammasome in FoxO6-KO liver

To investigate the role of FoxO6 in glucose metabolism, Calabuig-Navarro et al. [30] employed a breeding strategy to pro-

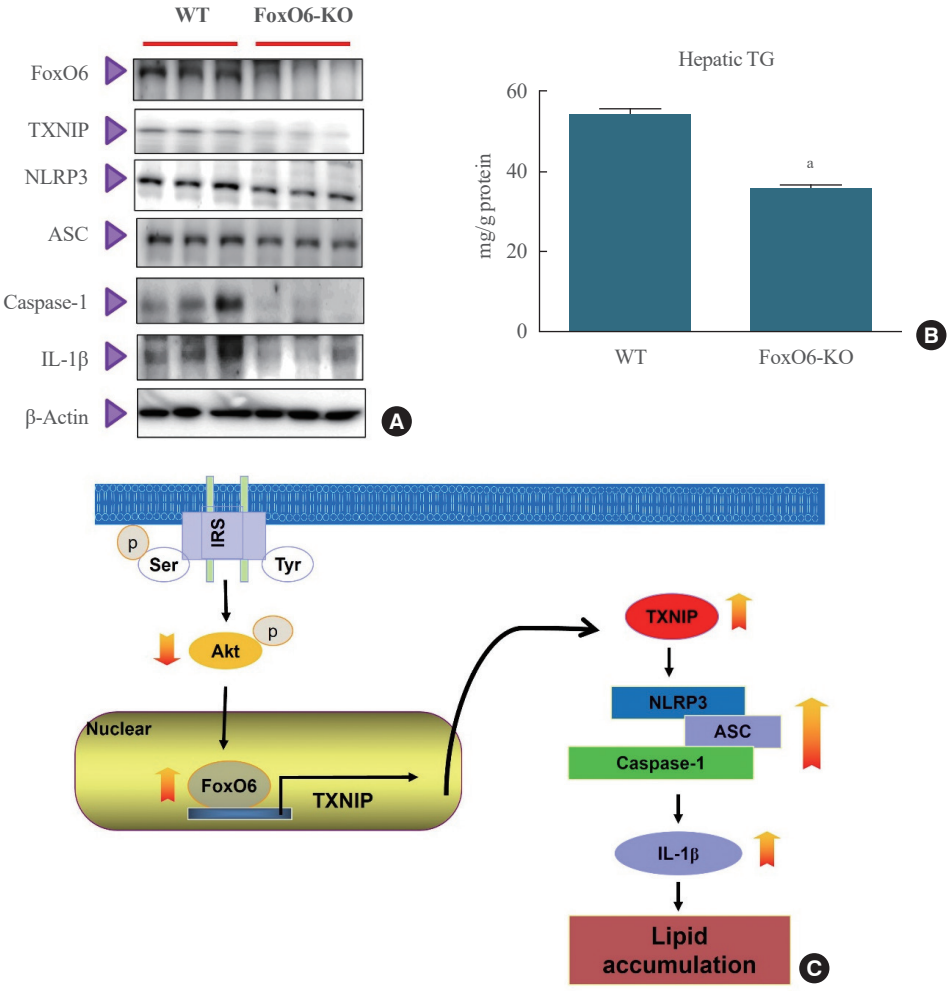

Fig. 6. Changes in the nucleotide-binding oligomerization domain-like receptor pyrin domain-containing-3 (NLRP3) inflammasome in response to forkhead box O6 (FoxO6) depletion. (A) Western blot was used to detect FoxO6, thioredoxin-interacting protein (TXNIP), NLRP3, apoptotic speck protein containing a caspase recruitment domain (ASC), caspase-1, and interleukin (IL)-1β in liver tissues; β-actin levels were used as loading controls. (B) The expression of relevant genes (FoxO6, insulin receptor substrate 1 [IRS1], IRS2, and IL-1β) was analyzed by quantitative polymerase chain reaction. The results were normalized with respect to actin levels. (C) Possible mechanism by which FoxO6 activates the NLRP3 inflammasome in insulin resistance. WT, wild-type; KO, knockout; TG, triglyceride; p, phospho; Ser, serine; Tyr, tyrosine; Akt, protein kinase B. [a]$P<0.001$ vs. WT by paired t test.

duce mice with a homozygous KO of the FoxO6 gene. These FoxO6-KO mice were viable and, when compared to wild-type control mice, exhibited markedly lower fasting blood glucose levels. Additionally, the FoxO6-KO mice demonstrated significantly enhanced blood glucose profiles during glucose tolerance tests.

To determine the impact of FoxO6 depletion on systemic inflammation, we measured the levels of the NLRP3 inflammasome. We observed significant differences in the levels of the proinflammatory cytokine IL-1β between FoxO6 KO mice and their wild-type littermates when fed a high-fat diet. Additionally, we evaluated the NLRP3 inflammasome levels using Western blot analysis. The results showed that NLRP3 inflammasome levels were lower in FoxO6-KO mice than in their wild-type littermates (Fig. 6A). Interestingly, hepatic triglyceride levels were also significantly lower in FoxO6-KO mice, as shown in Fig. 6B. To further investigate the role of FoxO6, we studied its ability to induce IL-1β expression in HepG2 cells. FoxO6 was found to be involved in the binding to and activation of the IL-1β promoter. This was confirmed by an IL-1β luciferase assay conducted on cells transduced with either an empty vector, a vector containing FoxO6, or a vector containing FoxO6-siRNA (Supplemental Fig. S3). Our findings suggest that FoxO6 depletion may lead to systemic inflammation in FoxO6-KO mice.

DISCUSSION

The primary contribution of our research is the novel identification of an interaction between FoxO6 and TXNIP, indicating that FoxO6 competes with its target genes. This finding is particularly intriguing because FoxO1, another FoxO family member, has been previously identified as a differential regulator of TXNIP expression in neurons [31] and in glucose-treated endothelial cells [22]. However, the role of FoxO6 in TXNIP regulation was not well understood until now. TXNIP has been recognized as a FoxO target gene [32] and functions as a tumor suppressor. Yamaguchi et al. [33] reported that the TXNIP-FoxO axis was involved in cell cycle arrest. Our recent studies revealed that FoxO6 was deregulated in the insulin-resistant liver, leading to a significant increase in both mRNA and protein expression in hepatocytes from dietary obese mice and diabetic *db/db* mice [11], which is associated with increased lipid metabolism [34].

Recent reports have indicated that the expression of NLRP3 inflammasome-related genes is associated with insulin resistance and obesity-induced impaired glucose tolerance [35]. Additionally, activation of these genes has been observed in the hepatocytes of mice [36]. The activation of the NLRP3 inflammasome is implicated in the pathophysiological processes leading to visceral obesity and insulin resistance. Other recent studies have demonstrated that NLRP3 knockout mice exhibit improved insulin sensitivity, evidenced by increased phosphorylation of insulin receptor substrate-1 and Akt in the liver and muscle [12,37]. Our findings support the notion that in the insulin-resistant liver, FoxO6 activity is abnormally elevated.

One of our aims in the current study was to shed light on the molecular interactions linking insulin resistance to the aberrant production of the proinflammatory cytokine IL-1β in liver cells. Our findings indicate that FoxO6 mediates the relationship between the abnormal production of proinflammatory cytokine IL-1β and the development of insulin resistance in liver cells (Fig. 3). Previous research has demonstrated that activation of the phosphoinositide 3-kinase (PI3K)/Akt pathway can effectively reduce palmitate-induced inflammatory cytokine production; however, the underlying regulatory mechanism remains uncharacterized [38,39]. In this study, we demonstrate that IL-1β expression is regulated by FoxO6, a crucial nuclear transcription factor that modulates the suppressive effects of insulin on target gene expression. In the absence of insulin, FoxO6 is localized in the nucleus, where it facilitates the expression of target genes. Conversely, in the presence of insulin, FoxO6 undergoes phosphorylation by Akt, leading to its exclusion from the nucleus and contributing to the repression of target gene expression.

This phosphorylation-dependent protein trafficking mechanism plays a major role in the ability of insulin to regulate the transcriptional activity of FoxO6 in cells [2,3,9]. Despite the association of insulin resistance with low-grade inflammation in obesity and type 2 diabetes, the precise mechanism underlying this association remains elusive. However, our data (Fig. 5B) indicate that the binding of FoxO6 to the TXNIP promoter may play a role in the relationship between insulin resistance and low-grade inflammation. Our study is the first to show that insulin resistance and palmitate can activate the TXNIP/NLRP3 inflammasome signaling pathway, which was associated with the release of IL-1β in mouse liver cells and HepG2 cells. These findings shed light on the cellular and molecular relationship between FoxO6 and TXNIP, proposing a novel target for diabetes treatment.

In conclusion, the binding of FoxO6 to TXNIP plays a significant role in linking hepatic steatosis with NLRP3-induced production of the proinflammatory cytokine IL-1β, both *in vivo* and

in vitro (Fig. 6C). Future research will concentrate on exploring the potential applications of these findings in preventing diabetes and its associated complications.

CONFLICTS OF INTEREST

No potential conflict of interest relevant to this article was reported.

ACKNOWLEDGMENTS

We thank Dr. H. Henry Dong (Children's Hospital of Pittsburgh of UPMC, Pittsburgh, PA, USA) for providing liver tissues from FoxO6-KO mice. This research was also supported by the Basic Science Research Program through the National Research Foundation of Korea (NRF), funded by the Ministry of Education (NRF-2021R1I1A1A01052055).

AUTHOR CONTRIBUTIONS

Conception or design: D.H.K. Acquisition, analysis, or interpretation of data: M.E.K., J.S.L., T.W.K., M.H.P., D.H.K. Drafting the work or revising: M.H.P., D.H.K. Final approval of the manuscript: M.E.K., J.S.L., T.W.K., M.H.P., D.H.K.

ORCID

Mi Eun Kim *https://orcid.org/0000-0002-3815-5126*
Min Hi Park *https://orcid.org/0000-0002-6191-993X*
Dae Hyun Kim *https://orcid.org/0000-0003-4391-5502*

REFERENCES

1. Van Der Heide LP, Hoekman MF, Smidt MP. The ins and outs of FoxO shuttling: mechanisms of FoxO translocation and transcriptional regulation. Biochem J 2004;380(Pt 2):297-309.
2. Accili D, Arden KC. FoxOs at the crossroads of cellular metabolism, differentiation, and transformation. Cell 2004;117:421-6.
3. Barthel A, Schmoll D, Unterman TG. FoxO proteins in insulin action and metabolism. Trends Endocrinol Metab 2005;16:183-9.
4. Biggs WH 3rd, Meisenhelder J, Hunter T, Cavenee WK, Arden KC. Protein kinase B/Akt-mediated phosphorylation promotes nuclear exclusion of the winged helix transcription factor FKHR1. Proc Natl Acad Sci U S A 1999;96:7421-6.
5. Kawamori D, Kaneto H, Nakatani Y, Matsuoka TA, Matsuhisa M, Hori M, et al. The forkhead transcription factor Foxo1 bridges the JNK pathway and the transcription factor PDX-1 through its intracellular translocation. J Biol Chem 2006;281:1091-8.
6. Martinez SC, Tanabe K, Cras-Meneur C, Abumrad NA, Bernal-Mizrachi E, Permutt MA. Inhibition of Foxo1 protects pancreatic islet beta-cells against fatty acid and endoplasmic reticulum stress-induced apoptosis. Diabetes 2008;57:846-59.
7. Hotamisligil GS. Inflammation and metabolic disorders. Nature 2006;444:860-7.
8. Schenk S, Saberi M, Olefsky JM. Insulin sensitivity: modulation by nutrients and inflammation. J Clin Invest 2008;118:2992-3002.
9. Kamagate A, Dong HH. FoxO1 integrates insulin signaling to VLDL production. Cell Cycle 2008;7:3162-70.
10. Kim DH, Lee B, Lee J, Kim ME, Lee JS, Chung JH, et al. FoxO6-mediated IL-1β induces hepatic insulin resistance and age-related inflammation via the TF/PAR2 pathway in aging and diabetic mice. Redox Biol 2019;24:101184.
11. Kim DH, Perdomo G, Zhang T, Slusher S, Lee S, Phillips BE, et al. FoxO6 integrates insulin signaling with gluconeogenesis in the liver. Diabetes 2011;60:2763-74.
12. Vandanmagsar B, Youm YH, Ravussin A, Galgani JE, Stadler K, Mynatt RL, et al. The NLRP3 inflammasome instigates obesity-induced inflammation and insulin resistance. Nat Med 2011;17:179-88.
13. Donath MY. Targeting inflammation in the treatment of type 2 diabetes: time to start. Nat Rev Drug Discov 2014;13:465-76.
14. Schroder K, Tschopp J. The inflammasomes. Cell 2010;140:821-32.
15. Febbraio MA. Role of interleukins in obesity: implications for metabolic disease. Trends Endocrinol Metab 2014;25:312-9.
16. Hoque R, Vodovotz Y, Mehal W. Therapeutic strategies in inflammasome mediated diseases of the liver. J Hepatol 2013;58:1047-52.
17. Chen J, Saxena G, Mungrue IN, Lusis AJ, Shalev A. Thioredoxin-interacting protein: a critical link between glucose toxicity and beta-cell apoptosis. Diabetes 2008;57:938-44.
18. Perrone L, Devi TS, Hosoya K, Terasaki T, Singh LP. Thioredoxin interacting protein (TXNIP) induces inflammation through chromatin modification in retinal capillary endothe-

lial cells under diabetic conditions. J Cell Physiol 2009;221:262-72.
19. Zhou R, Tardivel A, Thorens B, Choi I, Tschopp J. Thioredoxin-interacting protein links oxidative stress to inflammasome activation. Nat Immunol 2010;11:136-40.
20. Minn AH, Hafele C, Shalev A. Thioredoxin-interacting protein is stimulated by glucose through a carbohydrate response element and induces beta-cell apoptosis. Endocrinology 2005;146:2397-405.
21. Parikh H, Carlsson E, Chutkow WA, Johansson LE, Storgaard H, Poulsen P, et al. TXNIP regulates peripheral glucose metabolism in humans. PLoS Med 2007;4:e158.
22. Li X, Rong Y, Zhang M, Wang XL, LeMaire SA, Coselli JS, et al. Up-regulation of thioredoxin interacting protein (Txnip) by p38 MAPK and FOXO1 contributes to the impaired thioredoxin activity and increased ROS in glucose-treated endothelial cells. Biochem Biophys Res Commun 2009;381:660-5.
23. Stoltzman CA, Peterson CW, Breen KT, Muoio DM, Billin AN, Ayer DE. Glucose sensing by MondoA:Mlx complexes: a role for hexokinases and direct regulation of thioredoxin-interacting protein expression. Proc Natl Acad Sci U S A 2008;105:6912-7.
24. Kim DH, Kim JY, Yu BP, Chung HY. The activation of NF-kappaB through Akt-induced FOXO1 phosphorylation during aging and its modulation by calorie restriction. Biogerontology 2008;9:33-47.
25. Laemmli UK. Cleavage of structural proteins during the assembly of the head of bacteriophage T4. Nature 1970;227:680-5.
26. Schulze PC, Yoshioka J, Takahashi T, He Z, King GL, Lee RT. Hyperglycemia promotes oxidative stress through inhibition of thioredoxin function by thioredoxin-interacting protein. J Biol Chem 2004;279:30369-74.
27. Nivet-Antoine V, Cottart CH, Lemarechal H, Vamy M, Margaill I, Beaudeux JL, et al. trans-Resveratrol downregulates Txnip overexpression occurring during liver ischemia-reperfusion. Biochimie 2010;92:1766-71.
28. Chutkow WA, Patwari P, Yoshioka J, Lee RT. Thioredoxin-interacting protein (Txnip) is a critical regulator of hepatic glucose production. J Biol Chem 2008;283:2397-406.
29. Boaru SG, Borkham-Kamphorst E, Tihaa L, Haas U, Weiskirchen R. Expression analysis of inflammasomes in experimental models of inflammatory and fibrotic liver disease. J Inflamm (Lond) 2012;9:49.
30. Calabuig-Navarro V, Yamauchi J, Lee S, Zhang T, Liu YZ, Sadlek K, et al. Forkhead box O6 (FoxO6) depletion attenuates hepatic gluconeogenesis and protects against fat-induced glucose disorder in mice. J Biol Chem 2015;290:15581-94.
31. Al-Mubarak B, Soriano FX, Hardingham GE. Synaptic NMDAR activity suppresses FOXO1 expression via a cis-acting FOXO binding site: FOXO1 is a FOXO target gene. Channels (Austin) 2009;3:233-8.
32. Xuan Z, Zhang MQ. From worm to human: bioinformatics approaches to identify FOXO target genes. Mech Ageing Dev 2005;126:209-15.
33. Yamaguchi F, Hirata Y, Akram H, Kamitori K, Dong Y, Sui L, et al. FOXO/TXNIP pathway is involved in the suppression of hepatocellular carcinoma growth by glutamate antagonist MK-801. BMC Cancer 2013;13:468.
34. Kim DH, Zhang T, Lee S, Calabuig-Navarro V, Yamauchi J, Piccirillo A, et al. FoxO6 integrates insulin signaling with MTP for regulating VLDL production in the liver. Endocrinology 2014;155:1255-67.
35. Goossens GH, Blaak EE, Theunissen R, Duijvestijn AM, Clement K, Tervaert JW, et al. Expression of NLRP3 inflammasome and T cell population markers in adipose tissue are associated with insulin resistance and impaired glucose metabolism in humans. Mol Immunol 2012;50:142-9.
36. Csak T, Ganz M, Pespisa J, Kodys K, Dolganiuc A, Szabo G. Fatty acid and endotoxin activate inflammasomes in mouse hepatocytes that release danger signals to stimulate immune cells. Hepatology 2011;54:133-44.
37. Wen H, Gris D, Lei Y, Jha S, Zhang L, Huang MT, et al. Fatty acid-induced NLRP3-ASC inflammasome activation interferes with insulin signaling. Nat Immunol 2011;12:408-15.
38. Guha M, Mackman N. The phosphatidylinositol 3-kinase-Akt pathway limits lipopolysaccharide activation of signaling pathways and expression of inflammatory mediators in human monocytic cells. J Biol Chem 2002;277:32124-32.
39. Molnarfi N, Gruaz L, Dayer JM, Burger D. Opposite regulation of IL-1beta and secreted IL-1 receptor antagonist production by phosphatidylinositide-3 kinases in human monocytes activated by lipopolysaccharides or contact with T cells. J Immunol 2007;178:446-54.